

## TOPICAL REVIEW

# Tactile and temperature sensors based on organic transistors: Towards e-skin fabrication

Miao Zhu<sup>1</sup>, Muhammad Umair Ali<sup>2,3</sup>, Changwei Zou<sup>1</sup>, Wei Xie<sup>1</sup>, Songquan Li<sup>1</sup>, Hong Meng<sup>3,†</sup><sup>1</sup>*School of Physical Science and Technology, Lingnan Normal University, Zhanjiang 524048, China*<sup>2</sup>*Department of Materials Science and Engineering, College of Engineering, Peking University, Beijing 100871, China*<sup>3</sup>*School of Advanced Materials, Peking University Shenzhen Graduate School, Peking University, Shenzhen 518055, China*Corresponding author. E-mail: <sup>†</sup>[menghong@pku.edu.cn](mailto:menghong@pku.edu.cn)

Received July 21, 2020; accepted August 8, 2020

Tactile and temperature sensors are the key components for e-skin fabrication. Organic transistors, a kind of intrinsic logic devices with diverse internal configurations, offer a wide range of options for sensor design and have played a vital role in the fabrication of e-skin-oriented tactile and temperature sensors. This research field has attained tremendous advancements, both in terms of materials design and device architecture, thereby leading to excellent performance of resulting tactile/temperature sensors. Herein, a systematic review of organic transistor-based tactile and temperature sensors is presented to summarize the latest progress in these devices. Particularly, we focus on spotlighting various device structures, underlying mechanisms and their performance. Lastly, an outlook for the future development of these devices is briefly discussed. We anticipate that this review will provide a quick overview of such a rapidly emerging research direction and attract more dedicated efforts for the development of next-generation sensing devices towards e-skin fabrication.

**Keywords** tactile sensor, temperature sensor, flexible, e-skin, organic transistor

## Contents

1	Introduction	1
2	Tactile sensors	2
2.1	Capacitive-type tactile sensors	2
2.2	Piezoelectric-type tactile sensors	4
2.3	Resistive-type tactile sensors	4
2.4	Other types of tactile sensors	5
3	Temperature sensors	6
3.1	Integrated organic transistor-based temperature sensors	6
3.2	Intrinsic organic transistor-based temperature sensors	9
4	Conclusion and perspectives	10
	Acknowledgements	10
	References	10

evolve more and more closely to a real human in near future. However, without strong sensing capability of human skin, the “hard” body of a robot is more like to be just the exoskeleton of crabs. Lately, the development of micro-nano materials and sensors makes it possible to incorporate massive and a variety of sensors in the robot’s body to enhance the sensing ability. Furthermore, the rise of conductive polymers [1–3] and advances in the booming research on flexible electronics [4–7] gave birth to the electronic skin (e-skin). e-skin is a kind of electronic device that can bionically imitate the skin of human beings. Robots comprising e-skin can interact with human and environment more effectively, just like a real body of human beings. Besides, e-skin with enough compliance, flexibility, and high sensitivity can be applied directly on the human skin as a wearable device to enhance its sensation to environmental stimuli.

Tactile and temperature sensing are two of the most important and basic functions of an e-skin. Among extensive reports on e-skin-oriented sensors, there are two main types of devices to realize tactile and temperature sensing: resistor-type (including, impedance and any response that results from the change in resistance in non-transistor-based devices), and transistor-type. Resistor-type sensors are based on a pressure or temperature sensitive resistor that could respond to pressure/temperature stimulus. To meet the needs of e-skin fabrication, usu-

## 1 Introduction

From the ages of World War I, efforts to develop robots that could help (even replace) human beings to perform tough tasks have been continuously increasing which led to the realization of intelligent machines that tend to

\*Special Topic: Organic Semiconductors and OFETs (Eds. Hong Meng & Guangcun Shan).

ally, the materials for such resistor application can be conductive two-dimensional (2D), like graphene [8–12] and transition-metal carbide/carbonitride (MXene) [13–15], or more commonly, composites of inorganic conductive materials and flexible organic matrices [16–19]. The resistor-type sensors benefit from their simple structure and mechanism, but they are not capable for the post-processing of input signal of pressure or temperature. Compared with the resistor-type, transistor-type counterparts can respond to the pressure or temperature stimulus with real-time logic control by the on/off status of a transistor, which is quite effective for the integration of e-skin-based intelligent circuits or systems. Typically, the active materials applied in the fabrication of tactile/temperature sensitive transistors include inorganic 2D [20–25], organic [26–30], and inorganic/organic composite semiconductors [31, 32]. Compared with 2D semiconductors, organic materials possess innumerable structures with plentiful properties, which offer a wide range of options for transistor design. Furthermore, most of the organic materials exhibit excellent flexibility, and the overall performance of organic transistors can be conveniently modulated by both molecular and structural design. Thus, after years of development, organic transistors now demonstrate encouraging prospects for e-skin fabrication. Tactile and temperature sensors based on organic transistors (TTS-OT) can be classified into several typical categories, as schematically illustrated in Fig. 1.

Herein, historical evolution and recent progress of TTS-OT are systematically reviewed, especially focusing on their structures, mechanism and performance. Finally, considering the current status and challenges in this research field, a brief outlook is provided for the future development of organic transistor-based high-performance

tactile/temperature sensors.

## 2 Tactile sensors

Tactile sensing is one of the basic functions of human skin. From the perspective of bionics, tactile sensing is indispensable for e-skin fabrication, which is mainly realized via incorporating tactile sensors. The mechanism of organic transistors-based tactile sensors can be generally classified into three types: capacitive-type, piezoelectric-type and resistive-type [36–39], as described in the following sections. It is to be noted that research on organic transistor-based sensors has garnered tremendous attention in recent years, and several articles that provide a systematical review of the history and development of this field have been published [40–45]. Thus, herein, we mainly focus on the latest research advancements reported in the past three years.

### 2.1 Capacitive-type tactile sensors

The dielectric layer of an organic transistor can be regarded as a parallel plate capacitor, and the capacitance satisfies the following equation [36]:

$$C = \frac{\varepsilon_0 \varepsilon_r S}{d}, \quad (1)$$

where  $C$ ,  $\varepsilon_0$ ,  $\varepsilon_r$ ,  $S$ , and  $d$  correspond to capacitance, permittivity of vacuum, relative dielectric constant, area of the parallel electrode plates and distance between the two electrode plates, respectively. Apparently, the pressure stimulus exerted on a transistor can lead to the deformation of dielectric layer, i.e., the area and distance between

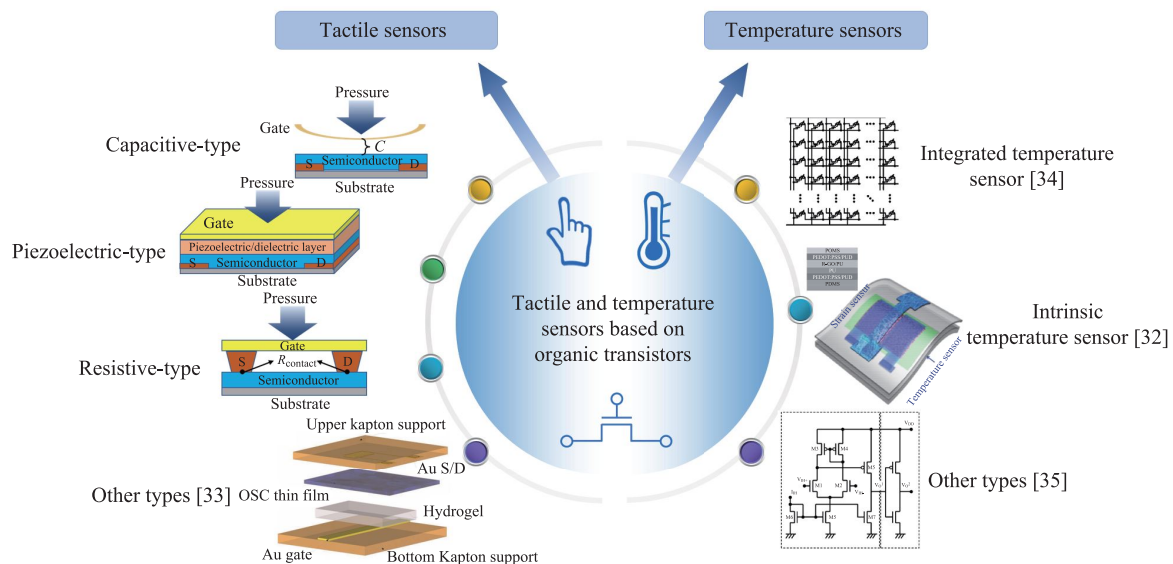


**Fig. 1** Various types of TTS-OT [32–35]. Reproduced with permission from Refs. [32–35].

the two electrode plates will be consequently changed, thereby causing a variation in the capacitance of dielectric layer. Capacitance is strongly related to the output characteristics of transistors, so the capacitive-type organic transistor-based tactile sensors can detect the tactile pressure signal via the capacitance change of the dielectric layer of a transistor.

The typical structure of capacitive-type organic transistors is a suspended gate configuration. In this structure, a narrow air-gap exists between the gate electrode and the active layer; the shape of this air-gap will change upon exerting pressure stimulus on the device, resulting in a capacitance change of the air-gap. Usually, applied pressure will reduce the vertical distance of air-gap, thereby increasing the capacitance and effective gate voltage which causes an increase in the current between source and drain electrodes. Sun and co-workers developed a capacitive-type organic transistor-based tactile sensor that works on this mechanism [Fig. 2(a)] [46]. High- $k$   $\text{Al}_2\text{O}_3$  dielectric layer was printed on a flexible poly(ethylene terephthalate) (PET) substrate by a roller printer with a thickness range of 12.4–23.9 nm. By incorporating with a tin doped indium oxide (ITO)/poly(ethylene terephthalate) (PET) extended suspending gate electrode, the or-

ganic transistor-based device exhibited high pressure sensitivity ( $8 \text{ kPa}^{-1}$ ), fast response time ( $<100 \text{ ms}$ ) and low operation voltage ( $-2 \text{ V}$ ). Yin *et al.* fabricated a capacitive-type organic transistor-based pressure sensor with the same structure and mechanism [47]. In their work, poly(methyl methacrylate) (PMMA)/ polyacrylic acid (PAA) bilayer as a dielectric layer is proposed to improve the transistor characteristics by decreasing the operation voltage, suppressing the hysteresis and reducing the leakage current. After the introduction of same ITO/PET suspending gate voltage, the device showed a super-high pressure sensitivity of  $56.15 \text{ kPa}^{-1}$  at low operation voltage ( $-5 \text{ V}$ ). Contrary to the suspended gate structure, a new type of capacitive tactile sensor was designed by Yin and colleagues via modulating the contact area between parallel-plate electrodes and the dielectric material, elastic ionic polyacrylamide hydrogel (EIPH) [Fig. 2(b)] [48]. EIPH was patterned as a pillar-like structure and placed between the two ITO/PET substrates to form a parallel plate capacitive pressure sensor element. Once the capacitor is pressed, the top of the EIPH pillar is deformed and the contact area of the ITO/PET and EIPH is increased, resulting in a capacitance enhancement and current response to the pressure.

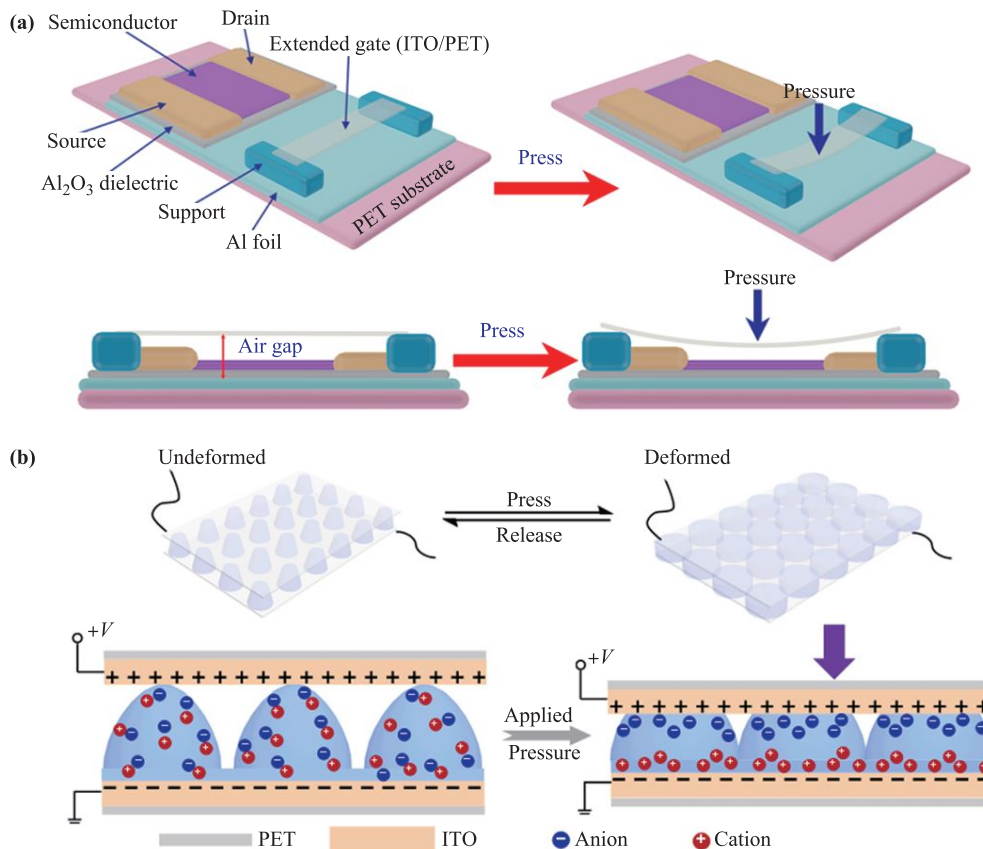


**Fig. 2** Schematics of typical capacitive-type organic transistor-based tactile sensors. (a) Air-gap-based capacitive tactile sensor with  $\text{Al}_2\text{O}_3$  dielectric layer. (b) Contact area controlled capacitive tactile sensor. Reproduced with permission from Ref. [46] (a) and Ref. [48] (b).

## 2.2 Piezoelectric-type tactile sensors

Piezoelectric effect is an intrinsic property of piezoelectric materials which can convert pressure to electricity directly through an electric polarization process. By incorporating a piezoelectric material into organic transistors as the functional dielectric layer, the resulting device will be able to respond to the tactile signal with a change in current due to the charge modulation caused by the piezoelectric effect.

Poly(vinylidene difluoride) (PVDF) is a widely used flexible piezoelectric organic material which is quite suitable for transistor fabrication. Ogunleye and co-workers developed a dual-gate organic transistor tactile sensor by laminating a layer of PVDF-trifluoroethylene (TrFE) on the 6,13-bis(triisopropylsilylethynyl) (TIPS)-pentacene/polystyrene channel [Fig. 3(a)] [49]. Owing to the piezoelectric effect of PVDF-TrFE, a pressure-induced voltage can be generated when pressure is exerted on the corresponding device. This will cause a shift in the threshold voltage of the transistor and thereby respond to the pressure stimulus. Viola and collaborators also proposed a PVDF-TrFE-based organic transistor pressure/temperature bimodal sensor [Fig. 3(b)] [50]. Although their device structure is bit different, the mechanism of pressure sensing is still based on the charge variation caused by the PVDF-TrFE piezoelectric effect. The device could work at a low operation voltage of  $-5$  V and respond to pressure robustly in the range of 1–5 N. Besides, Xu's group developed a lead zirconate titanate (PZT) piezoelectric ceramic-based organic transistor bimodal sensor [Fig. 3(c)] [51]. According to the similar mechanism as reported in the aforementioned works, the

as-fabricated device showed obvious response to natural tapping on its surface.

## 2.3 Resistive-type tactile sensors

Resistive-type tactile sensors work on the change in conductivity or resistance during charge transportation between source and drain (S/D) electrodes upon the application of pressure on a device. A typical structure to realize the resistive response to the pressure is to pattern the S/D electrodes which should be deformable enough to cause some variation in the contact resistance as a result of applied pressure. As designed by Baek and collaborators [Fig. 4(a)] [52], poly(dimethylsiloxane) (PDMS) embedded with single-walled carbon nanotubes (SWCNTs) was patterned to develop pyramid shape array that worked as deformable S/D electrodes of a transistor-based pressure sensor. The contact area between the pyramid PDMS/SWCNT electrodes and the semiconductor would increase when pressure is exerted, resulting in a significant reduction of the contact resistance, thereby leading to a high pressure sensitivity ( $18.96$  kPa $^{-1}$ ). Likewise, Wang and colleagues used Au-coated pyramid-type PDMS electrodes and dinaphtho [2,3-b:2',3'-f] thieno [3,2-b] thiophene (DNTT) organic semiconductor to fabricate a highly sensitive pressure sensor [Fig. 4(b)] [53]. The device showed excellent sensitivity as high as  $514$  kPa $^{-1}$ , low limit of detection (10 Pa) and fast response time (1.8 ms). Instead of patterned pyramid electrodes as mentioned above, Liu and co-workers directly used an ITO coated PET sheet as flexible top gate electrode of a transistor pressure sensor [Fig. 4(c)] [54]. The ITO/PET sheet showed bending when pressure was applied on it, which

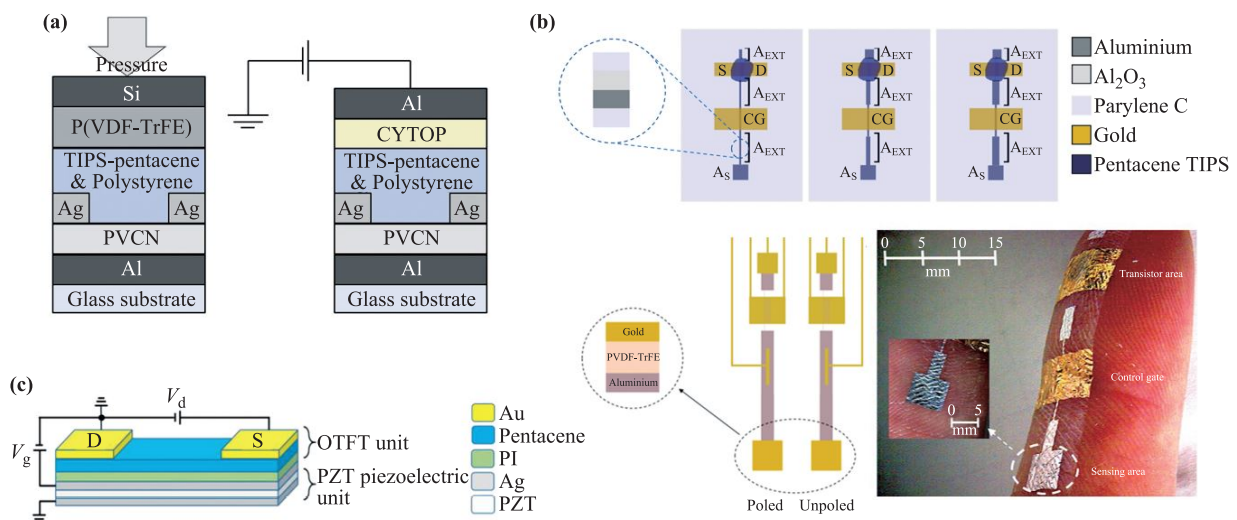


**Fig. 3** Schematics of typical piezoelectric-type organic transistor-based tactile sensors. (a) P(VDF-TrFE)-based piezoelectric tactile sensor. (b) Piezoelectric tactile sensor with physically separated sensing and amplification elements. (c) PZT piezoelectric ceramic-based organic transistor tactile sensor. Reproduced with permission from Ref. [49] (a), Ref. [50] (b) and Ref. [51] (c).

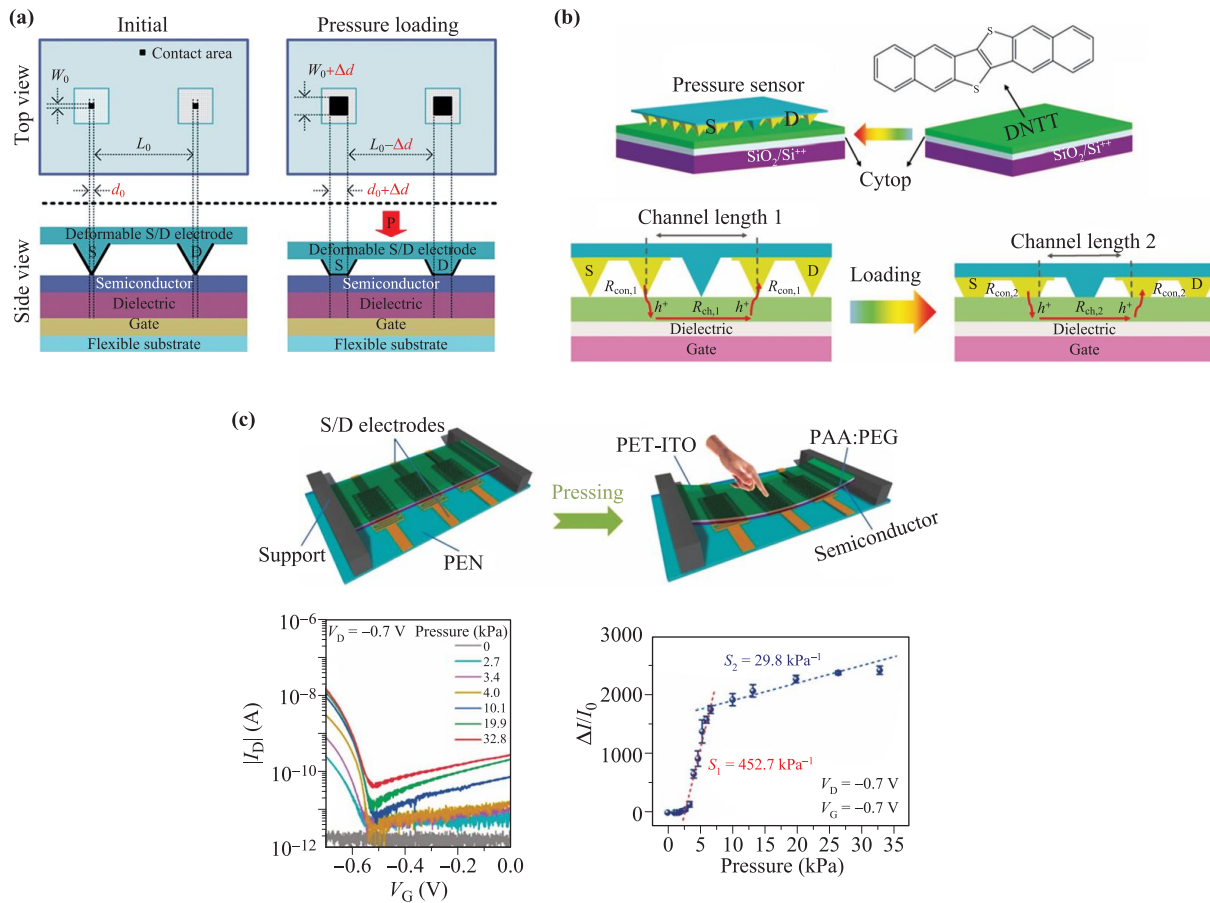


**Fig. 4** Schematics of typical resistive-type organic transistor tactile sensors. (a) A piezoelectric tactile sensor based on pyramid shaped S/D electrodes. The contact resistance varies according to the shape change when pressure is exerted. (b) A DNNT-based resistive transistor tactile sensor that works on the same mechanism as of (a). (c) Resistive transistor tactile sensor based on the control of contact resistance between flexible active layer and the electrodes. Reproduced with permission from Ref. [52] (a), Ref. [53] (b), and Ref. [54] (c).

led to a change in the pressure-dependent contact interface area between the gate and semiconductor. Therefore, the drain current responds to the pressure according to the similar mechanism as elaborated above. Especially, by using PAA:poly(ethyleneglycol) (PEG) dielectric layer, the device achieved a high sensitivity ( $452.7 \text{ kPa}^{-1}$ ) at an extremely low operation voltage of  $-0.7$  V.

#### 2.4 Other types of tactile sensors

Certainly, tactile sensing can be realized by various mechanisms. Zhang *et al.* developed a new type of water dipole-based transistor pressure sensor [33]. The transistor was fabricated by introducing a layer of water-based hydrogel between the gate and semiconductor layer. The hydrogel layer could reduce the operation voltage as well as minimize the requisite pressure through pressure-induced orientation change of water molecule dipoles. The device exhibited large response range, from several hundred Pa to 9 kPa, and high sensitivity at a low operation voltage

of less than 0.5 V. Triboelectric-type sensors have been developed as an important type of tactile sensors that work on the basis of triboelectric charges and their transfer during a touch-separation process [55–57]. This type of sensors is mainly known for self-powered working mode and high sensitivity. The key component of such devices is a triboelectric nanogenerator (TENG) which is generally constructed by organic materials. Some of the TENGs can be incorporated into transistors to form triboelectric-type transistor tactile sensors, as the device developed by Wang's group and depicted in Fig. 5 [58]. TENG consists of a pair of frictional layers: a Kapton negative-charge receiving layer and an aluminum positive-charge residual layer. Each of them could work as a mobile layer to receive external forces. When an external force is applied on or released from the mobile layer, an electron flow between source and mobile electrode will be induced by the triboelectric-charge-field to form a tactile sensitive inner electric field, which is equivalent to the gate voltage and enables the device to sensitively respond to the tactile

**Table 1** Characteristics and device parameters of recently reported organic transistor-based tactile sensors.

Type*	Semiconductor**	Mobility ( $\text{cm}^2 \cdot \text{V}^{-1} \cdot \text{s}^{-1}$ )	Operation voltage	Sensitivity	Pressure range	Detection limit	Response time
C [46]	Pentacene	0.65	-2 V	$8 \text{ kPa}^{-1}$	0-14 kPa	500 Pa	<100 ms
C [47]	PIDT-BT:TCNQ	0.11	-5 V	$56.15 \text{ kPa}^{-1}$	0-32.8 kPa	/	<20 ms
C [48]	PIDT-BT:TCNQ PTB7-Th	/	2 V	$12.64 \text{ kPa}^{-1}$ $17.95 \text{ kPa}^{-1}$	0-1.5 kPa	/	540 ms
P [49]	TIPS-Pentacene/Polystyrene	0.8	/	/	0-451 kPa	/	/
P [50]	TIPS-Pentacene	/	/	/	1-5 N	/	/
P [51]	Pentacene	$4.81 \times 10^{-3}$	0-0.9 V	/	/	/	/
R [52]	DPP-DTT	/	-1.2 V	$18.96 \text{ kPa}^{-1}$	0-38.7 kPa	12 Pa	140 ms
R [53]	DNTT	1-2	-5-60 V	$514 \text{ kPa}^{-1}$	0-1 kPa	10 Pa	1.8 ms
R [54]	PIDT-BT:TCNQ	0.56	-0.7 V	$452.7 \text{ kPa}^{-1}$	0-32.8 kPa	200 Pa	57.9 ms
O [58]	p-Si	/	5 V	/	/	/	/
O [33]	diF-TES-ADT:PS	0.8	<0.5 V	$\sim 10 \text{ mV} \cdot \text{kPa}^{-1}$	0.3-9 kPa	/	2000 ms
C [59]	PIDT-BT:TCNQ	4.65	-3 V	$691.9 \text{ kPa}^{-1}$	0-33.43 kPa	13.3 Pa	19.4 ms
R [60]	DNTT	0.3-2.45	-5 V	/	/	/	/
P [61]	TIPS-Pentacene/Polystyrene	$\sim 0.3$	0	/	/	/	/
P [62]	DNTT	0.02-0.56	/	$\sim 65 \text{ mV} \cdot \text{N}^{-1}$	0-9 N	/	/
R [63]	29-DPP-SVS/SEBS	$\sim 1.37$	10-30 V	/	/	/	/
P [64]	TIPS-Pentacene	$\sim 0.07$	/	$25 \text{ nA} \cdot \text{g}^{-1}$	0-1 kPa	/	/

\*C, R, P, and O refer to capacitive-type, resistive-type, piezoelectric-type and other types of organic transistor-based tactile sensors, respectively.

\*\*See detailed structures in the corresponding references.

signals.

The characteristics and device parameters of recently reported (since 2018 and onwards) organic transistor tactile sensors are summarized in Table 1. It should be noted that some works just demonstrated the potential of corresponding devices in tactile sensor application without systematic measurements, so we could not add some of

the parameters in the table.

### 3 Temperature sensors

Compared to tactile sensors, there are quite a few reports on organic transistors-based temperature sensors, especially in the case of single mode temperature sensors. More commonly, temperature sensing element is integrated in a bimodal sensor which can work as both tactile and temperature sensors.

#### 3.1 Integrated organic transistor-based temperature sensors

As a matter of fact, organic transistor-based temperature sensors have been developed in the very early stage of research on e-skin-inspired organic transistor sensors. Someya and group designed an integrated bimodal sensor by integrating thermal and pressure sensing modules into a transistor array (Fig. 6) [65].

The thermal sensing unit in their device was composed of a copper phthalocyanine (CuPc)/3,4,9,10-perylenetetracarboxylic-diimide (PTCDI) diode, while the

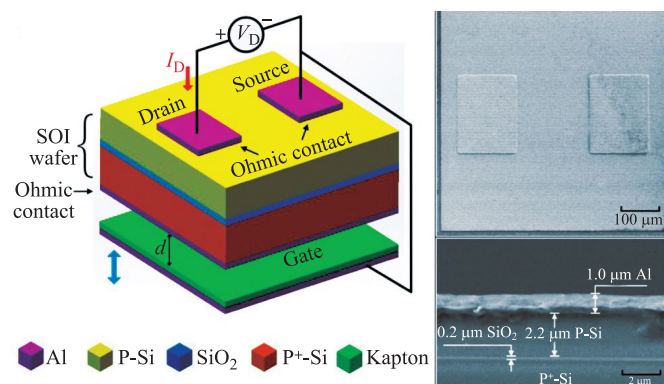


**Fig. 5** A triboelectric-type tactile sensor based on a transistor with TENG. Reproduced with permission from Ref. [58].

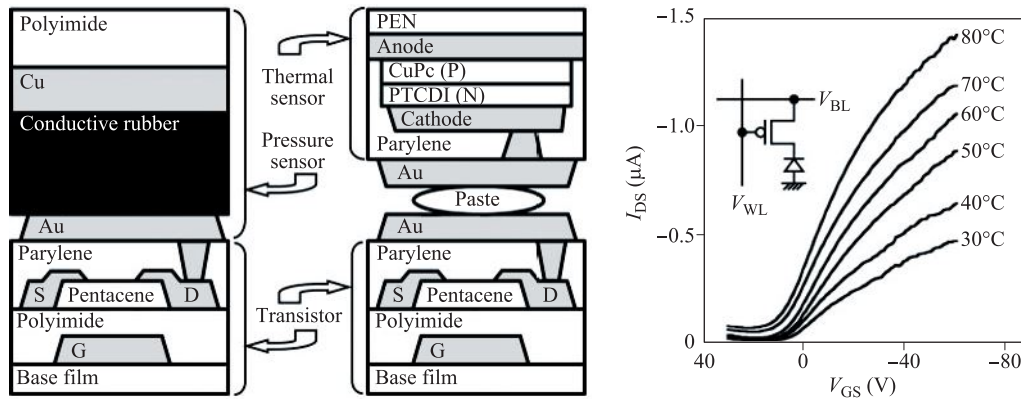


**Fig. 6** Schematic and temperature response of organic transistor-based bimodal sensor with a CuPc/PTCDI diode temperature sensing element. Reproduced with permission from Ref. [65].

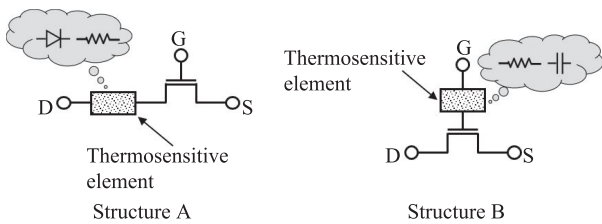


**Fig. 7** Typical structures of integrated organic transistor-based temperature sensors. Structure A: The thermosensitive element is located between S/D electrodes and the active layer; Structure B: The thermosensitive element located between gate electrode and the active layer.

pressure sensor component was based on a conductive rubber.

The sensing and transistor modules were pasted together in order to sense the thermal and pressure signals with the logic circuit constructed by organic transistor array. Generally, the skeleton of these devices can be described as a frame of “thermosensitive elements + transistor” (Fig. 7). The thermosensitive elements can either be located at S/D terminal (structure A) or at gate terminal (structure B). Theoretically, the thermosensitive elements

in structure A can be a thermosensitive diode or a thermistor, while in structure B, it can be a thermal sensitive capacitor or a thermistor, too.

Apparently, the device described above adopts structure A. In contrast, Graz and co-workers combined an organic transistor with layers of polymers embedded with piezoelectric ceramic and pyroelectric particles on a flexible substrate to construct a flexible bimodal organic transistor sensor using structure B [Fig. 8(a)] [66]. The temperature or pressure stimulus could lead to a variation in carriers of the sensing element which worked as a charge source parallel to the sensor capacitance, enabling the current response to temperature and pressure. The piezoelectric/pyroelectric sensing mechanism simplified the device structure to a certain extent, but it seems still complex compared to the intrinsic transistor sensor. Certainly, the mechanism of the sensing element is varied. Ren and co-workers proposed a thermistor temperature sensing element composed of Ag nanoparticles (NPs) and pentacene [67]. The strong temperature dependence of the thermistor led to a high dynamic range of the whole device after it was integrated into an organic transistor. Due to the outstanding temperature sensing properties of Ag NPs/pentacene thermistor, it was further applied in

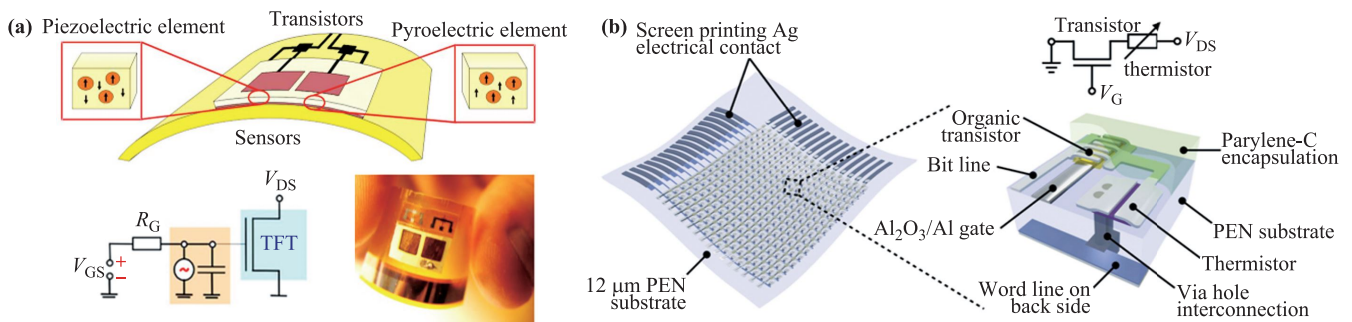


**Fig. 8** Organic transistor-based temperature sensors with (a) pyroelectric sensing element and (b) Ag NPs/pentacene thermistor sensing element. Reproduced from Refs. [34, 66].

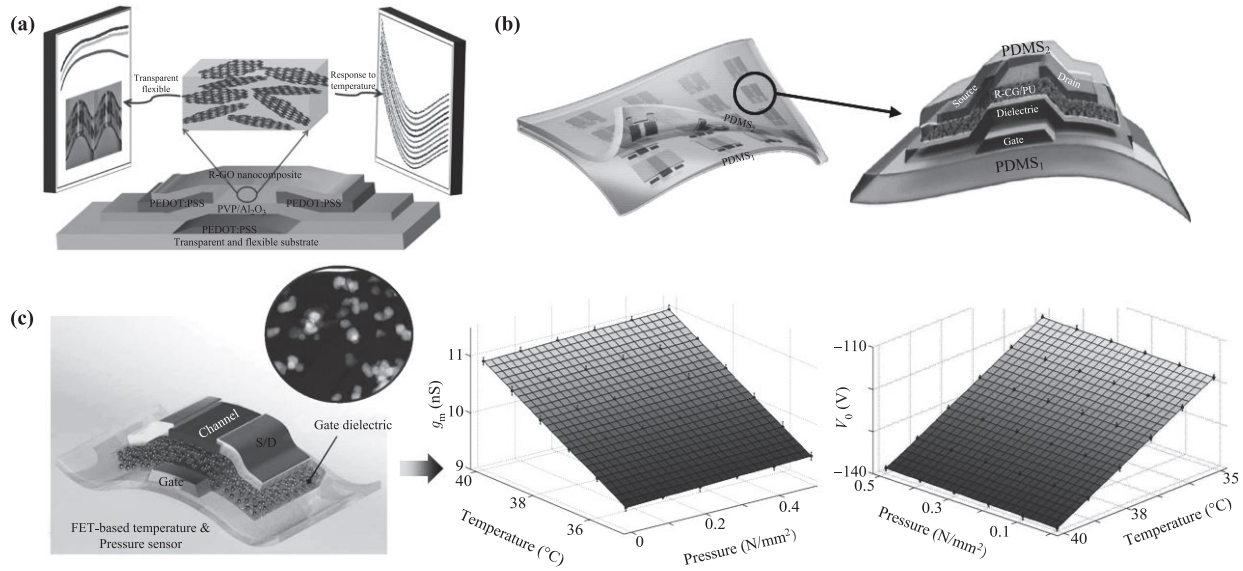


**Fig. 9** Intrinsic organic transistor temperature/bimodal sensors based on (a) rGO/P(VDF-TrFE), (b) rGO/PU and (c) pentacene. Reproduced with permission from Ref. [31] (a), Ref. [32] (b), and Ref. [69] (c).

an organic transistor array with DNTT active layer and  $\text{Al}_2\text{O}_3$ /self-assembled monolayer (SAM) dielectric to realize a flexible, large-area and low operating power organic transistor-based temperature sensor [Fig. 8(b)] [34].

Different from traditional thermopiles and pyroelectric temperature sensing mechanism, Zhao *et al.* developed a new concept of thermosensitive element based on ionic thermoelectric effects [68]. The large Seebeck coefficient ( $\sim 10^4 \mu\text{V}\cdot\text{K}^{-1}$ ) of the polymer electrolyte ionic ther-

moelectric material, poly(vinylphosphonic acid-co-acrylic acid) (P(VPA-AA)), could enable a much higher amplification ( $\sim 10^3$  times) of the temperature response than the devices based on traditional thermoelectric sensing elements.

The integrated organic transistor-based temperature sensors exhibit good flexibility with excellent response to thermal stimulus, and can be directly integrated in various flexible electronic devices. However, the overall structure

**Table 2** Characteristics and device parameters of recently reported organic transistor-based tactile sensors.

Type*	Semiconductor**	Mobility ( $\text{cm}^2\cdot\text{V}^{-1}\cdot\text{s}^{-1}$ )	Sensitivity	Temperature range	Detection limit
I [65]	Pentacene	1	/	30–160 °C	/
I [66]	$\alpha$ -Si:H	0.66	/	/	/
I [34]	Pentacene	/	/	/	/
I [34]	DNTT	$\sim 0.5$	0.044 (TCR)***	20–100 °C	0.4 °C
I [68]	P3HT	/	$\sim 104 \mu\text{V}\cdot\text{K}^{-1}$ (Seebeck coefficient)	15–45 °C ( $\Delta T$ )	/
I [73]	Pentacene	0.25–1.46	/	20–50 °C	0.0043 °C
II [31]	rGO/P(VDF-TrFE)	$\sim 0.006$	$\sim 2.483 \times 10^{-7} \text{ A}\cdot\text{K}^{-1}$	30–80 °C	0.1 °C
II [32]	rGO/PU	/	1.34% °C $^{-1}$	30–80 °C	0.2 °C
II [69]	Pentacene	$\sim 0.00768$	/	25–70 °C	/
II [70]	PDPPFT4	$\sim 0.21$	$-2.89\% \text{ }^\circ\text{C}^{-1}$	25–55 °C	1 °C
	PII2T	$\sim 0.28$	$-4.23\% \text{ }^\circ\text{C}^{-1}$		1.5 °C
II [71]	Pentacene	0.146	/	20–100 °C	/
III [72]	CuPc	0.004	/	–23–97 °C	/
III [35]	C10-DNBDT	3	$-0.87\% \text{ }^\circ\text{C}^{-1}$	20–80 °C	/
	GSID 104031-1 (BASF SE)	0.1	0.064% °C $^{-1}$ (Cr/Au)		

\*I, II and III represent the integrated-type, intrinsic-type and other types of temperature sensors based on organic transistors, respectively.

\*\*See detailed structures of the semiconductors in corresponding references.

\*\*\*TCR refers to the temperature coefficient of resistance, which is defined by  $\text{TCR} = R^{-1} dR/dT$  [34].

of such devices still remains complicated. On the other hand, intrinsic organic transistor-based temperature sensor, which can sense the temperature by itself without any additional sensing elements provides a good solution to this issue.

### 3.2 Intrinsic organic transistor-based temperature sensors

Semiconductors play a crucial role in the development of intrinsic organic transistor-based temperature sensors. During the early stages, 2D materials were typically combined with organic semiconductors to form a composite active material for the transistor channel. Lee's group synthesized copolymers by adding reduced graphene oxide (rGO) sheets into P(VDF-TrFE) [Fig. 9(a)] [31] and polyurethane (PU) [Fig. 9(b)] [32] to fabricate sensitive all-elastomeric flexible bimodal sensors. The as-fabricated devices exhibited excellent temperature response performance. The rGO/PU-based device was able to indicate the temperature change of skin effectively upon drinking warm water. However, the channel composed of massive reduced graphene sheets was discontinuous microscopically; the high contact resistance between the graphene sheets and large amounts of structural defects led to the low mobility ( $\sim 10^{-3} \text{ cm}^2 \cdot \text{V}^{-1} \cdot \text{s}^{-1}$ ) of these devices. Meanwhile, pentacene, a widely used organic semiconductor, was also used to fabricate a bimodal sensor based on a similar structure by the same team [Fig. 9(c)] [69]. In this work, a general approach to fabricate e-skin-oriented bimodal organic transistor sensors was proposed, which enables real-time sensing and extracts different effects (for example, temperature and pressure) from multiple stimuli.

Unlike integrated temperature sensors, it is hard to improve the performance of intrinsic temperature sensors by structural modifications. A practical way is to design more effective molecules for the active layer. Zhu and co-workers synthesized two typical organic semiconductors, poly(diketopyrrolopyrrole-[3,2-b]thieno[2',3':4,5]thieno[2,3-]thiophene) (PDPPFT4) and poly(isoindigo-bithiophene) (PII2T), which were deposited on polystyrene-block-poly(ethylene-ran-butylene)-block-polystyrene (SEBS) with azide-crosslinker dielectric layer as the active materials for organic transistor-based temperature sensor [70]. The as-fabricated devices exhibited reliable stretchability and temperature dependence in a temperature range of 25–55°C.

Till now, most of the reported flexible organic transistor-based temperature sensors are fabricated on polymer substrates. Although these substrates can provide excellent flexibility and high mechanical strength, the large thermal resistance severely reduces the accuracy of temperature sensor and delays the response time. In order to resolve this problem, Meng's group developed an organic transistor-based temperature sensor on a piece of commercial graphite paper which man-

ifested both super-high thermal conductivity and enough mechanical strength as an efficient flexible substrate [Fig. 10(a)] [71]. The as-fabricated device exhibited high linearity in a wide temperature range from 20 to 100 °C with nearly hysteresis-free transfer characteristics, which greatly expanded the potential substrate materials for the fabrication of flexible organic transistor sensors. Since graphite paper has been widely used as thermal conductive material in modern electronic devices, graphite paper-containing organic transistor-based temperature sensor offers convenience and great potential for integration in such devices as an accurate and fast temperature sensing component.

Finally, it should be mentioned that there are indeed some other types of organic transistor-based temperature sensors that operate under totally different mechanism. Subbarao and co-workers found that the hysteresis of an organic thin-film transistor based on PMMA/poly(vinyl alcohol) (PVA)/Al<sub>2</sub>O<sub>3</sub> dielectric layer and CuPc active layer was sensitive to temperature in a range of –23–

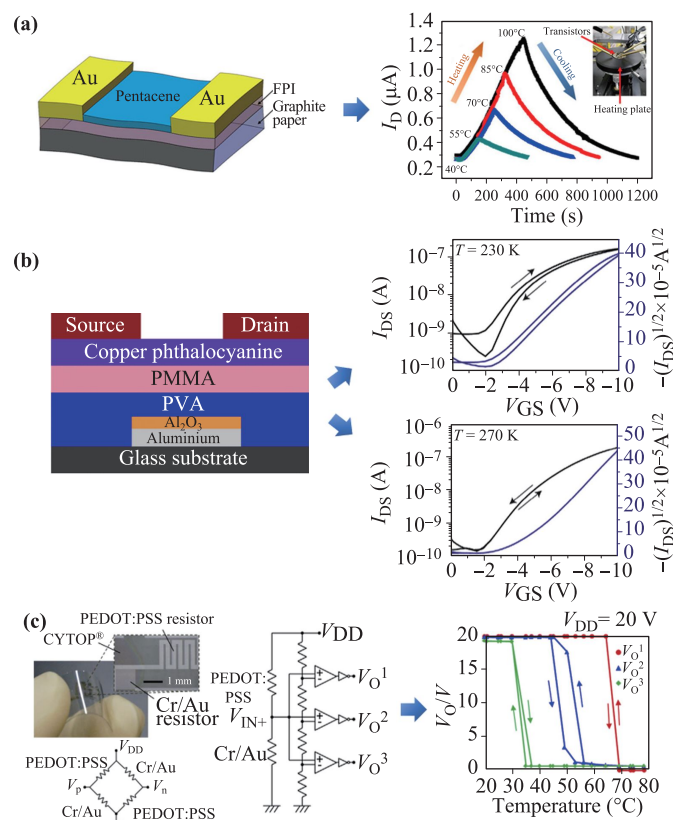


**Fig. 10** (a) Flexible organic transistor-based temperature sensor fabricated on commercial graphite paper substrate. (b) An organic transistor temperature sensor based on hysteresis-dependence temperature change. (c) A digital-output organic transistor-based temperature sensor that adopts a Wheatstone bridge temperature sensor and organic comparator. Reproduced from Ref. [71] (a), Ref. [72] (b), and Ref. [35] (c).

97 °C, which can be used as a temperature sensor and monitor [Fig. 10(b)] [72]. Nakayama and collaborators integrated a Wheatstone bridge temperature sensor composed of Cr/Au metal resistors and PEDOT:PSS organic resistors into a P/N organic transistor comparator to realize a digital-output temperature sensor [Fig. 10(c)] [35]. The diverse variety of such working mechanisms greatly enriches the types of organic transistor-based temperature sensors and facilitate their integration into various electronic systems.

The characteristics and device parameters of typical organic transistor-based temperature sensors are presented in Table 2.

## 4 Conclusion and perspectives

In summary, tactile and temperature sensors are critical components for e-skin fabrication. After years of research and evolution, the performance of TTS-OT has been greatly improved and the underlying operation mechanism of these devices can be categorized in several typical modes. Most of the organic transistor-based tactile sensors work on the pressure-induced change of capacitance, charge modulation and resistance, corresponding to the capacitive-type, piezoelectric-type and resistive-type tactile sensors, respectively. Whereas, organic transistor-based temperature sensors can be classified in two typical models, including integrated and intrinsic temperature sensors. Although they work under different mechanisms, there is no obvious evidence that indicates the sensitivity or other parameters of these sensors are directly associated with their type. Hence, these sensors can be adopted for e-skin design and fabrication without any discrimination. Instead of the device type, materials (especially, applied as the dielectric layer) play an important role in reducing the operation voltage and power consumption of a transistor sensor. By innovation in materials synthesis and optimization of dielectric layer structure, the operation voltage has been reduced to less than 0.5 V till now. As the research in this area is intensifying, we believe that transistor sensors with low power consumption will emerge in the future. Furthermore, organic light-emitting diodes and other real-time display elements are being integrated into various flexible sensors [74–78], which would enable a transistor sensor to work as an independent device in a more complicated e-skin-based systems.

**Acknowledgements** This work was supported by the Characteristic Innovation Projects of General Colleges and Universities in Guangdong Province (Grant No. 2018KTSCX132), the Natural Science Foundation of Guangdong Province (Grant Nos. 2018A030307027 and 2020A1515011488), the Natural Science Research Special Foundation of Lingnan Normal University (Grant No. ZL2045), the Major Projects of Basic and Application Research in Guangdong Province (Grant No. 2017KZDXM055), the Special Fund for Science and Technology Innovation Strategy of Guang-

dong Province (Grant No. 2018A03015), and Zhanjiang Science and Technology Plan (Grant No. 2018A02010).

## References

1. T. Nezakati, A. Seifalian, A. Tan, and A. M. Seifalian, Conductive polymers: Opportunities and challenges in biomedical applications, *Chem. Rev.* 118(14), 6766 (2018)
2. J. Chen, Q. Yu, X. Cui, M. Dong, J. Zhang, C. Wang, J. Fan, Y. Zhu, and Z. Guo, An overview of stretchable strain sensors from conductive polymer nanocomposites, *J. Mater. Chem. C* 7(38), 11710 (2019)
3. J. Chen, Y. Zhu, J. Huang, J. Zhang, D. Pan, J. Zhou, J. Ryu, A. Umar, and Z. Guo, Advances in responsively conductive polymer composites and sensing applications, *Polym. Rev.*, doi:10.1080/15583724.2020.1734818 (2020)
4. C. H. Lee, B. Kim, and K. Kim, Printing flexible and hybrid electronics for human skin and eye-interfaced health monitoring systems, *Adv. Mater.* 32(15), 1902051 (2019)
5. H. R. Lim, H. S. Kim, R. Qazi, Y. T. Kwon, J. W. Jeong, and W. H. Yeo, Advanced soft materials, sensor integrations, and applications of wearable flexible hybrid electronics in healthcare, energy, and environment, *Adv. Mater.* 32(15), 1901924 (2020)
6. W. Gao, H. Ota, D. Kiriya, K. Takei, and A. Javey, Flexible electronics toward wearable sensing, *Acc. Chem. Res.* 52(3), 523 (2019)
7. Y. Liu, M. Pharr, and G. A. Salvatore, Lab-on-skin: A review of flexible and stretchable electronics for wearable health monitoring, *ACS Nano* 11(10), 9614 (2017)
8. H. Xu, M. K. Zhang, Y. F. Lu, J. J. Li, S. J. Ge, and Z. Z. Gu, Dual-mode wearable strain sensor based on graphene/colloidal crystal films for simultaneously detection of subtle and large human motions, *Adv. Mater. Technol.* 5(2), 1901056 (2020)
9. X. You, J. Yang, M. Wang, J. Huh, Y. Ding, X. Zhang and S. Dong, Graphene-based fiber sensors with high stretchability and sensitivity by direct ink extrusion, *2D Mater.* 7(1), 015025 (2020)
10. C. Deng, P. Gao, L. Lan, P. He, X. Zhao, W. Zheng, W. Chen, X. Zhong, Y. Wu, L. Liu, J. Peng, and Y. Cao, Ultrasensitive and highly stretchable multifunctional strain sensors with timbre-recognition ability based on vertical graphene, *Adv. Funct. Mater.* 29(51), 1907151 (2019)
11. C. Yang, W. Liu, N. Liu, J. Su, L. Li, L. Xiong, F. Long, Z. Zou, and Y. Gao, Graphene aerogel broken to fragments for a piezoresistive pressure sensor with a higher sensitivity, *ACS Appl. Mater. Interfaces* 11(36), 33165 (2019)
12. B. Zhao, Y. Wang, S. Sinha, C. Chen, D. Liu, A. Dasgupta, L. Hu, and S. Das, Shape-driven arrest of coffee stain effect drives the fabrication of carbon-nanotube-graphene-oxide inks for printing embedded structures and temperature sensors, *Nanoscale* 11(48), 23402 (2019)

13. Y. Cheng, Y. Ma, L. Li, M. Zhu, Y. Yue, W. Liu, L. Wang, S. Jia, C. Li, T. Qi, J. Wang, and Y. Gao, Bioinspired microspines for a high-performance spray  $Ti_3C_2T_x$  MXene-based piezoresistive sensor, *ACS Nano* 14(2), 2145 (2020)
14. Y. Gao, C. Yan, H. Huang, T. Yang, G. Tian, D. Xiong, N. Chen, X. Chu, S. Zhong, W. Deng, Y. Fang, and W. Yang, Microchannel-confined MXene based flexible piezoresistive multifunctional micro-force sensor, *Adv. Funct. Mater.* 30(11), 1909603 (2020)
15. Z. Cao, Y. Yang, Y. Zheng, W. Wu, F. Xu, R. Wang, and J. Sun, Highly flexible and sensitive temperature sensors based on  $Ti_3C_2T_x$  (MXene) for electronic skin, *J. Mater. Chem. A* 7(44), 25314 (2019)
16. T. Huang, P. He, R. Wang, S. Yang, J. Sun, X. Xie, and G. Ding, Porous fibers composed of polymer nanoball decorated graphene for wearable and highly sensitive strain sensors, *Adv. Funct. Mater.* 29(45), 1903732 (2019)
17. Z. Zeng, S. I. S. Shahabadi, B. Che, Y. Zhang, C. Zhao, and X. Lu, Highly stretchable, sensitive strain sensors with a wide linear sensing region based on compressed anisotropic graphene foam/polymer nanocomposites, *Nanoscale* 9(44), 17396 (2017)
18. S. Riyajuddin, S. Kumar, S. P. Gaur, A. Sud, T. Maruyama, M. E. Ali, and K. Ghosh, Linear piezoresistive strain sensor based on graphene/g- $C_3N_4$ /PDMS heterostructure, *Nanotechnology* 31(29), 295501 (2020)
19. Q. Tian, W. Yan, Y. Li, and D. Ho, Bean pod-inspired ultrasensitive and self-healing pressure sensor based on laser-induced graphene and polystyrene microsphere sandwiched structure, *ACS Appl. Mater. Interfaces* 12(8), 9710 (2020)
20. R. Furlan de Oliveira, P. A. Livio, V. Montes-García, S. Ippolito, M. Eredia, P. Fanjul-Bolado, M. B. González García, S. Casalini, and P. Samori, Liquid-gated transistors based on reduced graphene oxide for flexible and wearable electronics, *Adv. Funct. Mater.* 29(46), 1905375 (2019)
21. Z. Wang, Z. Hao, S. Yu, C. G. D. Moraes, L. H. Suh, X. Zhao, and Q. Lin, An ultraflexible and stretchable aptameric graphene nanosensor for biomarker detection and monitoring, *Adv. Funct. Mater.* 29(44), 1905202 (2019)
22. N. Schaefer, R. G. Cortadella, J. Martneíz-Aguilar, G. Schwesig, X. Illa, A. M. Lara, S. Santiago, C. Hébert, G. Guirado, R. Villa, A. Sirota, A. Guimerà-Brunet, and J. A. Garrido, Multiplexed neural sensor array of graphene solution-gated field-effect transistors, *2D Mater.* 7(2), 025046 (2020)
23. T. Leng, K. Parvez, K. Pan, J. Ali, D. McManus, K. S. Novoselov, C. Casiraghi, and Z. Hu, Printed graphene/ $WS_2$  battery-free wireless photosensor on papers, *2D Mater.* 7(2), 024004 (2020)
24. L. Li, Y. Guo, Y. Sun, L. Yang, L. Qin, S. Guan, J. Wang, X. Qiu, H. Li, Y. Shang, and Y. Fang, A general method for the chemical synthesis of large-scale, seamless transition metal dichalcogenide electronics, *Adv. Mater.* 30(12), 1706215 (2018)
25. D. Zhang, J. Du, Y. L. Hong, W. Zhang, X. Wang, H. Jin, P. L. Burn, J. Yu, M. Chen, D. M. Sun, M. Li, L. Liu, L. P. Ma, H. M. Cheng, and W. Ren, A double support layer for facile clean transfer of two-dimensional materials for high-performance electronic and optoelectronic devices, *ACS Nano* 13(5), 5513 (2019)
26. P. W. M. Blom, Polymer electronics: To be or not to be? *Adv. Mater. Technol.* 5(6), 2000144 (2020) <https://doi.org/10.1002/admt.202000144>
27. K. G. Lim, E. Guo, A. Fischer, Q. Miao, K. Leo, and H. Kleemann, Anodization for simplified processing and efficient charge transport in vertical organic field-effect transistors, *Adv. Funct. Mater.* 2001703(27), 2001703 (2020)
28. S. Fratini, M. Nikolka, A. Salleo, G. Schweicher, and H. Sirringhaus, Charge transport in high-mobility conjugated polymers and molecular semiconductors, *Nat. Mater.* 19(5), 491 (2020)
29. H. Zhong, G. Wu, Z. Fu, H. Lv, G. Xu, and R. Wang, Flexible porous organic polymer membranes for protonic field-effect transistors, *Adv. Mater.* 32(21), 2000730 (2020)
30. H. Chen, W. Zhang, M. Li, G. He, and X. Guo, Interface engineering in organic field-effect transistors: Principles, applications, and perspectives, *Chem. Rev.* 120(5), 2879 (2020)
31. T. Q. Trung, S. Ramasundaram, S. W. Hong, and N. E. Lee, Flexible and transparent nanocomposite of reduced graphene oxide and P(VDF-TrFE) copolymer for high thermal responsivity in a field-effect transistor, *Adv. Funct. Mater.* 24(22), 3438 (2014)
32. T. Q. Trung, S. Ramasundaram, B. U. Hwang, and N. E. Lee, An all-elastomeric transparent and stretchable temperature sensor for body-attachable wearable electronics, *Adv. Mater.* 28(3), 502 (2016)
33. Q. Zhang, F. Leonardi, R. Pfattner, and M. Mas-Torrent, A solid-state aqueous electrolyte-gated field-effect transistor as a low-voltage operation pressure-sensitive Platform, *Adv. Mater. Interfaces* 6(16), 1900719 (2019)
34. X. Ren, K. Pei, B. Peng, Z. Zhang, Z. Wang, X. Wang, and P. K. L. Chan, A low-operating-power and flexible active-matrix organic-transistor temperature-sensor array, *Adv. Mater.* 28(24), 4832 (2016)
35. K. Nakayama, B. S. Cha, Y. Kanaoka, N. Isahaya, M. Omori, M. Uno, and J. Takeya, Organic temperature sensors and organic analog-to-digital converters based on p-type and n-type organic transistors, *Org. Electron.* 36, 148 (2016)
36. Y. H. Lee, M. Jang, M. Y. Lee, O. Y. Kweon, and J. H. Oh, Flexible field-effect transistor-type sensors based on conjugated molecules, *Chem* 3(5), 724 (2017)
37. K. Kim, G. Song, C. Park, and K. S. Yun, Multifunctional woven structure operating as triboelectric energy harvester, capacitive tactile sensor array, and piezoresistive strain sensor array, *Sensors* 17(11), 2582 (2017)
38. H. K. Kim, S. Lee, and K. S. Yun, Capacitive tactile sensor array for touch screen application, *Sens. Act. A: Phys.* 165(1), 2 (2011)

39. R. Surapaneni, Q. Guo, Y. Xie, D. J. Young, and C. H. Mastrangelo, A three-axis high-resolution capacitive tactile imager system based on floating comb electrodes, *J. Micromech. Microeng.* 23(7), 075004 (2013)
40. W. Shi, Y. Guo, and Y. Liu, When flexible organic field-effect transistors meet biomimetics: A prospective view of the internet of things, *Adv. Mater.* 32(15), 1901493 (2020)
41. Y. H. Lee, O. Y. Kweon, H. Kim, J. H. Yoo, S. G. Han, and J. H. Oh, Recent advances in organic sensors for health self-monitoring systems, *J. Mater. Chem. C* 6(32), 8569 (2018)
42. W. Gao, H. Ota, D. Kiriya, K. Takei, and A. Javey, Flexible electronics toward wearable sensing, *Acc. Chem. Res.* 52(3), 523 (2019)
43. X. Wu, S. Mao, J. Chen, and J. Huang, Strategies for improving the performance of sensors based on organic field-effect transistors, *Adv. Mater.* 30(17), 1705642 (2018)
44. D. Chen and Q. Pei, Electronic muscles and skins: A review of soft sensors and actuators, *Chem. Rev.* 117(17), 11239 (2017)
45. Y. Zang, D. Huang, C. Di, and D. Zhu, Device engineered organic transistors for flexible sensing applications, *Adv. Mater.* 28(22), 4549 (2016)
46. Q. J. Sun, T. Li, W. Wu, S. Venkatesh, X. H. Zhao, Z. X. Xu, and V. A. L. Roy, Printed high  $k$  dielectric for flexible low-power extended gate field-effect transistor in sensing pressure, *ACS Appl. Electron. Mater.* 1(5), 711 (2019)
47. Z. Yin, M. J. Yin, Z. Liu, Y. Zhang, A. P. Zhang, and Q. Zheng, Solution-processed bilayer dielectrics for flexible low-voltage organic field-effect transistors in pressure-sensing applications, *Adv. Sci.* 5(9), 1701041 (2018)
48. M. J. Yin, Z. Yin, Y. Zhang, Q. Zheng, and A. P. Zhang, Micropatterned elastic ionic polyacrylamide hydrogel for low-voltage capacitive and organic thin-film transistor pressure sensors, *Nano Energy* 58, 96 (2019)
49. O. O. Ogunleye, H. Sakai, Y. Ishii, and H. Murata, Investigation of the sensing mechanism of dual-gate low-voltage organic transistor based pressure sensor, *Org. Electron.* 75, 105431 (2019)
50. F. A. Viola, A. Spanu, P. C. Ricci, A. Bonfiglio, and P. Cosseddu, Ultrathin, flexible and multimodal tactile sensors based on organic field-effect transistors, *Sci. Rep.* 8(1), 8073 (2018)
51. Z. Meng, H. Zhang, M. Zhu, X. Wei, J. Cao, I. Murataza, M. U. Ali, H. Meng, and J. Xu, Lead zirconate titanate (a piezoelectric ceramic)-based thermal and tactile bimodal organic transistor sensors, *Org. Electron.* 80, 105673 (2020)
52. S. Baek, G. Y. Bae, J. Kwon, K. Cho, and S. Jung, Flexible pressure-sensitive contact transistors operating in the subthreshold regime, *ACS Appl. Mater. Interfaces* 11(34), 31111 (2019)
53. Z. Wang, S. Guo, H. Li, B. Wang, Y. Sun, Z. Xu, X. Chen, K. Wu, X. Zhang, F. Xing, L. Li, and W. Hu, The semiconductor/conductor interface piezoresistive effect in an organic transistor for highly sensitive pressure sensors, *Adv. Mater.* 31(6), 1805630 (2018)
54. Z. Liu, Z. Yin, J. Wang, and Q. Zheng, Polyelectrolyte dielectrics for flexible low-voltage organic thin-film transistors in highly sensitive pressure sensing, *Adv. Funct. Mater.* 29(1), 1806092 (2019)
55. Y. Yang, H. Zhang, Z. H. Lin, Y. S. Zhou, Q. Jing, Y. Su, J. Yang, J. Chen, C. Hu, and Z. L. Wang, Human skin based triboelectric nanogenerators for harvesting biomechanical energy and as self-powered active tactile sensor system, *ACS Nano* 7(10), 9213 (2013)
56. Z. Ren, J. Nie, L. Xu, T. Jiang, B. Chen, X. Chen, and Z. L. Wang, Directly visualizing tactile perception and ultrasensitive tactile sensors by utilizing body-enhanced induction of ambient electromagnetic waves, *Adv. Funct. Mater.* 28(47), 1805277 (2018)
57. R. Cao, X. Pu, X. Du, W. Yang, J. Wang, H. Guo, S. Zhao, Z. Yuan, C. Zhang, C. Li, and Z. L. Wang, Screen-printed washable electronic textiles as self-powered touch/gesture tribo-sensor for intelligent human-machine interaction, *ACS Nano* 12(6), 5190 (2018)
58. C. Zhang, W. Tang, L. Zhang, C. Han, and Z. L. Wang, Contact electrification field-effect transistor, *ACS Nano* 8(8), 8702 (2014)
59. Y. Jiang, Z. Liu, Z. Yin, and Q. Zheng, Sandwich structured dielectrics for air-stable and flexible low-voltage organic transistors in ultrasensitive pressure sensing, *Mater. Chem. Front.* 4(5), 1459 (2020)
60. D. Thuau, K. Begley, R. Dilmurat, A. Ablat, G. Wantz, C. Ayela, and M. Abbas, Exploring the critical thickness of organic semiconductor layer for enhanced piezoresistive sensitivity in field-effect transistor sensors, *Materials (Basel)* 13(7), 1583 (2020)
61. T. Ishikawa, H. Sakai, and H. Murata, Fabrication of the flexible dual-gate OFET based organic pressure sensor, *IEICE Trans. Elect.* E102-C(2), 188 (2019)
62. S. Hannah, A. Davidson, I. Glesk, D. Uttamchandani, R. Dahiya, and H. Gleskova, Multifunctional sensor based on organic field-effect transistor and ferroelectric poly(vinylidene fluoride trifluoroethylene), *Org. Electron.* 56, 170 (2018)
63. S. Wang, J. Xu, W. Wang, G. J. N. Wang, R. Rastak, F. Molina-Lopez, J. W. Chung, S. Niu, V. R. Feig, J. Lopez, T. Lei, S.K. Kwon, Y. Kim, A. M. Foudeh, A. Ehrlich, A. Gasperini, Y. Yun, B. Murmann, J. B.H. Tok, and Z. Bao, Skin electronics from scalable fabrication of an intrinsically stretchable transistor array, *Nature* 555(7694), 83 (2018)
64. S. Lai, F. A. Viola, P. Cosseddu, and A. Bonfiglio, Floating gate, organic field-effect transistor-based sensors towards biomedical applications fabricated with large-area processes over flexible substrates, *Sensors* 18(3), 688 (2018)

65. T. Someya, Y. Kato, T. Sekitani, S. Iba, Y. Noguchi, Y. Murase, H. Kawaguchi, and T. Sakurai, Conformable, flexible, large-area networks of pressure and thermal sensors with organic transistor active matrixes, *Proc. Natl. Acad. Sci. USA* 102(35), 12321 (2005)
66. I. Graz, M. Krause, S. Bauer-Gogonea, S. Bauer, S. P. Lacour, B. Ploss, M. Zirkl, B. Stadlober, and S. Wagner, Flexible active-matrix cells with selectively poled bifunctional polymer-ceramic nanocomposite for pressure and temperature sensing skin, *J. Appl. Phys.* 106(3), 034503 (2009)
67. X. Ren, P. K. L. Chan, J. Lu, B. Huang, and D. C. W. Leung, High dynamic range organic temperature sensor, *Adv. Mater.* 25(9), 1291 (2013)
68. D. Zhao, S. Fabiano, M. Berggren, and X. Crispin, Ionic thermoelectric gating organic transistors, *Nat. Commun.* 8(1), 14214 (2017)
69. N. T. Tien, S. Jeon, D. I. Kim, T. Q. Trung, M. Jang, B. U. Hwang, K. E. Byun, J. Bae, E. Lee, J. B. H. Tok, Z. Bao, N. E. Lee, and J. J. Park, A flexible bimodal sensor array for simultaneous sensing of pressure and temperature, *Adv. Mater.* 26(5), 796 (2014)
70. C. Zhu, H. C. Wu, G. Nyikayaramba, Z. Bao, and B. Murmann, Intrinsically stretchable temperature sensor based on organic thin-film transistor, *IEEE Electron Device Lett.* 40(10), 1630 (2019)
71. M. Zhu, J. Cao, X. Wei, Y. He, A. Li, X. Xu, M. U. Ali, L. Yan, and H. Meng, Self-supported hysteresis-free flexible organic thermal transistor based on commercial graphite paper, *Appl. Phys. Lett.* 112(25), 253301 (2018)
72. N. V. V. Subbarao, S. Mandal, M. Gedda, P. K. Iyer, and D. K. Goswami, Effect of temperature on hysteresis of dipolar dielectric layer based organic field-effect transistors: A temperature sensing mechanism, *Sens. Act. A: Phys.* 269, 491 (2018)
73. S. Mandal, M. Banerjee, S. Roy, A. Mandal, A. Ghosh, B. Satpati, and D. K. Goswami, Organic field-effect transistor-based ultrafast, flexible, physiological-temperature sensors with hexagonal barium titanate nanocrystals in amorphous matrix as sensing material, *ACS Appl. Mater. Interfaces* 11(4), 4193 (2019)
74. J. Jang, B. Oh, S. Jo, S. Park, H. S. An, S. Lee, W. H. Cheong, S. Yoo, and J. U. Park, Human-interactive, active-matrix displays for visualization of tactile pressures, *Adv. Mater. Technol.* 4(7), 1900082 (2019)
75. Y. H. Lee, O. Y. Kweon, H. Kim, J. H. Yoo, S. G. Han, and J. H. Oh, Recent advances in organic sensors for health self-monitoring systems, *J. Mater. Chem. C* 6(32), 8569 (2018)
76. S. Bi, Q. Li, Z. He, Q. Guo, K. Asare-Yeboah, Y. Liu, and C. Jiang, Highly enhanced performance of integrated piezo photo-transistor with dual inverted OLED gate and nanowire array channel, *Nano Energy* 66, 104101 (2019)
77. Y. J. Jeong, Y. E. Kim, K. J. Kim, E. J. Woo, and T. I. Oh, Multilayered fabric pressure sensor for real-time piezo-impedance imaging of pressure distribution, *IEEE Trans. Instrum. Meas.* 69(2), 565 (2020)
78. Y. Guo, M. Zhong, Z. Fang, P. Wan, and G. Yu, A wearable transient pressure sensor made with MXene nanosheets for sensitive broad-range human-machine interfacing, *Nano Lett.* 19(2), 1143 (2019)